ICHE 2014, Hamburg - Lehfeldt & Kopmann (eds) - © 2014 Bundesanstalt für Wasserbau ISBN 978-3-939230-32-8

Effects of Sediment Supply on Low-Flow Channel Formation

H. Miwa
National Institute of Technology, Maizuru College, Kyoto, Japan

ABSTRACT: Low-flow channels with pool and riffle sequences provide habitat for fish and vegetation during inter-flood periods. In regard to appropriate sediment management for river environments, it is important to investigate the effects of water discharge and sediment supply on the morphology of low-flow channels between floods. Such investigation can also provide information for investigating what controls on water discharge and sediment supply are better for the maintenance of riparian habitat. In this study, the effect of sediment supply on a low flow channel formation in alternate bars was investigated using flume experiments and two-dimensional numerical simulations. By investing river bed variation in detail, it was possible to clarify the formation process of emergent bars bounding a low-flow channel. The characteristics of the longitudinal profiles of low-flow channels were also investigated.

Keywords: Alternate bar, Low-flow channel, Emergent bar, Degradation, Sediment supply, Riffle and pool sequence, Numerical simulation

1 INTRODUCTION

Low-flow channels with pool and riffle sequences provide habitat for fish and vegetation during inter-flood periods. In regard to appropriate sediment management for river environments, it is important to investigate the effects of water discharge and sediment supply (both of which may be controlled by a dam as a water release and a sediment flushing from reservoirs) on the morphology of low-flow channels between floods. Such investigation can also provide information for investigating what controls on water discharge and sediment supply are better for the maintenance of riparian habitat. Many works on the river morphology change have mainly treated effects of the water discharge. However, effect of the sediment supply on the morphology change has not been always discussed.

Uchijima and Hayakawa (1987) investigated the low-flow channel formation and the local scour development caused by the alternate bar transformation under the low water discharge. Yuki et al. (1992) examined the phenomena similar to Uchijima and Hayakawa, and discussed the low-flow channel variation. These researches are mainly the studies on riverbed variations due to the decrease of water discharge. In addition, Shimizu et al. (2004) calculated the formation process of a low-flow channel in the bed with alternate bars under the dynamic equilibrium conditions through a numerical simulation. As mentioned above, the low-flow channel formation under a low water discharge has been investigated by some researchers. However, investigation on effects of sediment supply on the riverbed variation is not so many. This is because relationships between the bed degradation-aggradation and the bed form transformation are complex. Michiue et al. (1995) examined the effect of the presence of a sediment supply on the formation of low-flow channels under the double row bar formation conditions, and presented the numerical simulation method of that formation. Miwa et al. (2004a, b) investigated the effect of a water discharge on the low-flow channel deformation and the alternate bar formation in the uniform and the non-uniform sediment bed, and discussed the widening process of streambed and properties of wavelength and height. Miwa et al. (2007) also discussed the effects of rotational degradation/aggradation of riverbed caused by an imbalance between water and sediment discharge conditions on variation in alternate bar morphology. Takahata and Izumi (2011) performed the liner stability analysis incorporating

weakly non-equilibrium process of bed aggradation/degradation by use of the WKBJ method in order to clarify their effects. The analysis explained that riverbeds become stable and sand bars tend not to be formed under degradation, and that riverbeds become unstable under aggradation.

In this study, we investigated a low-flow channel formation process in alternate bars under the conditions with and without sediment supply using flume experiments, and discussed the effect of the sediment supply on that process. The two-dimensional numerical model was also applied to further investigate the effects of sediment supply on river restoration. The simulation results were verified against the experimental results. By investigating river bed variation in detail, it was possible to clarify the formation processes of emergent bars bounding a low-flow channel. Effects of the sediment supply on the longitudinal profiles of low-flow channels were also investigated.

2 FLUME EXPERIMENT (SET-UP AND PROCEDURE)

Experiments were conducted in a straight rectangular open channel with a length of 12 m, a width of 0.2 m and a depth of 0.3 m. Nearly uniform sediment was used in the experiments. The sediment has a mean grain diameter d_m of 0.110 cm, a geometric standard deviation σ_g $(=(d_{84}/d_{16})^{1/2}$, in which d_{84} and d_{16} are the grain sizes for which 84 % and 16 % of the sediment is finer, respectively) of 1.22 and specific gravity σ_s of 2.65.

The sand bed was flattened with a scraper, and was set to a slope of 0.0167 (1/60) before commencing experiment. At first, alternate bars were allowed to develop under the prescribed water discharge. The sediment was externally fed into the flow at the upstream end of the channel in order to keep the average bed level constant. After alternate bars had fully developed, water surface elevations were measured with a water level sensor at intervals of 20 cm in the longitudinal direction of the channel just before stopping the flow. Longitudinal profiles of the bed surface were measured with a laser sensor mounted on a self-propelled carriage, at intervals of 1 cm in the transverse direction of the channel after stopping the flow. The origin of the measurement (x=0) was set at a point of 3.65 m below the upstream of the channel; the measuring reach was from x=0 m to 7.95 m.

We investigated the processes of the alternate bar deformation and the low-flow channel formation by reducing the water discharge, next. Experiments were conducted with and without sediment supply. In the experiment with sediment supply, the sediment was fed into the flow in order to keep dynamic equilibrium of the bed. The position and shape of an individual emergent bar and the direction of sediment transport were sketched at any time during the experiment. The sediment discharge was specified by catching the sediment at the downstream end of the channel every 5 minutes. Water surface elevations and bed profiles were measured by the same as the above mentioned method. These measurements were repeated during the experiment. The stable alternate bars are the initial bed form in this study, and the origin of time is at the start of the experiment for the low-flow channel formation.

The experimental conditions for alternate bar development and low-flow channel formation are listed in Table 1. In the table, Q = water discharge, Q_{Bin} = sediment supply rate, h_m = mean flow depth, F_r = Froude number, τ_* = dimensionless bed shear stress $(= u_*^2/(\sigma/\rho\text{-}1)gd_m$, in which u_* = shear velocity, σ = sediment density, ρ = fluid density and g = gravity acceleration), L = mean wavelength, H = mean wave height and T = duration time of experiment.

Table 1. Experimental Conditions.

Status	Alternate bars								Low-flow channel		
Case	Q (cm^3/s)	Q_{Bin} (cm^3/s)	h_m (cm)	F_r	τ_*	L (cm)	H (cm)	T (min)	Q (cm^3/s)	Q_{Bin} (cm^3/s)	T (min)
US-1	800	200	1.18	1.00	0.104	71.9	1.51	56	300	50	590
US-0	800	200	1.16	1.02	0.102	63.2	1.50	57	300	0	575

3 NUMERICAL SIMULATION

3.1 *Outline of numerical model*

A two-dimensional shallow water model (Miwa and Parker, 2012) is applied to the simulation in this study. The outline of the model is described here. The continuity equation and the momentum equations in Cartesian coordinates are

$$\frac{\partial h}{\partial t}+\frac{\partial M}{\partial x}+\frac{\partial N}{\partial y}=0 \tag{1}$$

$$\frac{\partial M}{\partial t}+\frac{\partial uM}{\partial x}+\frac{\partial vM}{\partial y}=-gh\frac{\partial\left(h+z_b\right)}{\partial x}-\frac{\tau_{bx}}{\rho}+\frac{\partial}{\partial x}\left(-\overline{u'^2}h\right)+\frac{\partial}{\partial y}\left(-\overline{u'v'}h\right) \tag{2}$$

$$\frac{\partial N}{\partial t}+\frac{\partial uN}{\partial x}+\frac{\partial vN}{\partial y}=-gh\frac{\partial\left(h+z_b\right)}{\partial y}-\frac{\tau_{by}}{\rho}+\frac{\partial}{\partial x}\left(-\overline{u'v'}h\right)+\frac{\partial}{\partial y}\left(-\overline{v'^2}h\right) \tag{3}$$

where, M, N = discharge fluxes in x and y direction (M=uh, N=vh), u, v = velocity components in x and y direction, h = water depth, z_b = bed elevation, τ_{bx}, τ_{by} = bed shear stress components in x and y direction, and $-\overline{u'^2}$, $-\overline{u'v'}$, $-\overline{v'^2}$ = depth-averaged Reynolds stresses.

The bed shear stress components are written by using the velocity components with the following equations:

$$\tau_{bx}=\tau_b\frac{u}{\sqrt{u^2+v^2}},\quad \tau_{by}=\tau_b\frac{v}{\sqrt{u^2+v^2}} \tag{4a,b}$$

where τ_b = bed shear stress (= ρu_*^2). The shear velocity can be estimated by the Manning's equation.

The depth-averaged Reynolds stresses takes the following respective forms (e.g. Nagata et al., 2000);

$$-\overline{u'^2}=2\nu_t\left(\frac{\partial u}{\partial x}\right)-\frac{2}{3}k,\quad -\overline{u'v'}=\nu_t\left(\frac{\partial u}{\partial y}+\frac{\partial v}{\partial x}\right),\quad -\overline{v'^2}=2\nu_t\left(\frac{\partial v}{\partial y}\right)-\frac{2}{3}k \tag{5a,b,c}$$

$$\nu_t=\frac{\kappa}{6}u_*h,\quad k=2.07u_*^2 \tag{6a,b}$$

where ν_t = kinematic eddy viscosity, κ = Kármán constant (= 0.4) and k = depth averaged turbulent energy (Nezu and Nakagawa, 1993).

The continuity equation of sediment transport is

$$\frac{\partial z_b}{\partial t}+\frac{1}{1-\lambda}\left(\frac{\partial q_{Bx}}{\partial z}+\frac{\partial q_{By}}{\partial y}\right)=0 \tag{7}$$

where λ = bed porosity and q_{Bx}, q_{By} = sediment transport rates per unit width in x and y direction, respectively. The Ashida & Michiue equation (1972) and Hasegawa equation (1983) for sediment transport are employed in the model.

3.2 *Numerical simulation methods*

The governing equations are transformed into discrete forms with the finite volume method applied to staggered grids in a generalized coordinate system, and solved by the Euler explicit method. The advection terms are discretized by the TVD-MacCormack method. Rectangular coordinates are used in the simulation. The longitudinal grid size (Δx) is 0.1 m, and the lateral size (Δy) is 0.01 m. The time increment (Δt) is taken as 0.01 second for the flow calculation and as 0.1 second for the bed variation calculation. In the computation, the final bed profile of the experiment was used as the initial bed profile. The water discharge and water level are given at the upstream and downstream boundaries, respectively. The water discharge is given according to the following equation:

$$\frac{q}{q_m}=1+aR_n\left(y,t\right) \tag{8}$$

where q, q_m = water discharge and mean water discharge per unit width, respectively, a = constant for perturbation intensity, $R_n(y,t)$ = normal random number N(0,1), y = transverse direction, t = time. Figure 1 shows examples of the generation of normal random numbers and the water discharge variation due to perturbation. The constant (a) is taken as 0.1 in the simulation.

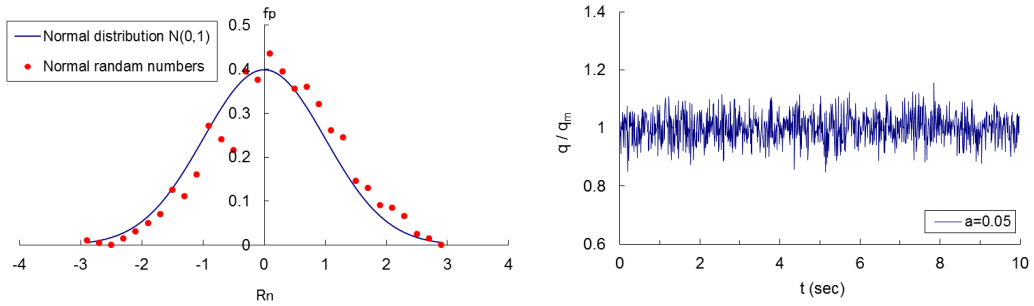

(a) Normal random number (b) Water discharge variation

Figure 1. Water discharge perturbation.

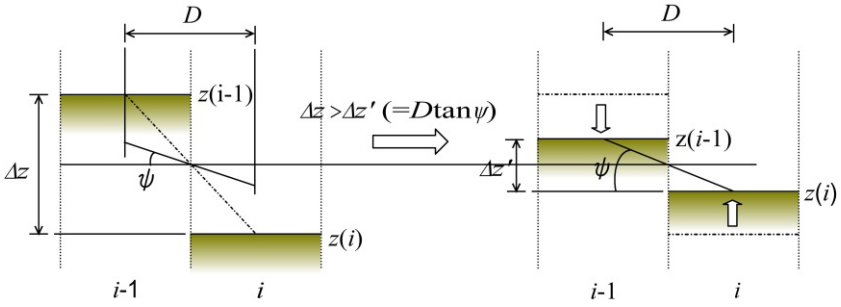

Figure 2. Conceptual diagram for bank erosion.

The bank erosion is dealt as follows in the simulation. Figure 2 shows the relevant conceptual diagram. That is, when the bed level difference between adjacent points, Δ_z, is larger than Δ_z' (= $D\tan\psi$; ψ=angle of repose), both bed levels changed as Fig.1. Then, the new bed elevations are given by

$$z(i) = z(i) + \frac{1}{2}\left(\Delta z - \Delta z'\right), \quad z(i-1) = z(i-1) + \frac{1}{2}\left(\Delta z - \Delta z'\right) \tag{9a,b}$$

The boundary between water and dry land is discriminated based on a threshold water depth. When the water depth of one grid node is less than or equal to the mean grain diameter of bed material, the grid is judged to be dry land. Only the pressure and bed shear stress terms are calculated in the momentum equation in order to track the boundary between water and dry land (Nagata, 1999).

4 LOW-FLOW CHANNEL FORMATION IN ALTERNATE BARS

4.1 *Effect of sediment supply on riverbed variation*

Figure 3 shows the temporal variations in transversely averaged longitudinal bed profile. The datum of the bed level is the transversely averaged bed at x =795 cm. The solid line indicates the bed profile of the stable alternate bars, which is the initial bed of the experiment for the low-flow channel formation. In the experiments, the bed profile of Case US-1 with sediment supply hardly varies during the experiments because of the balancing between the sediment discharge at the downstream end of the channel and the sedi-

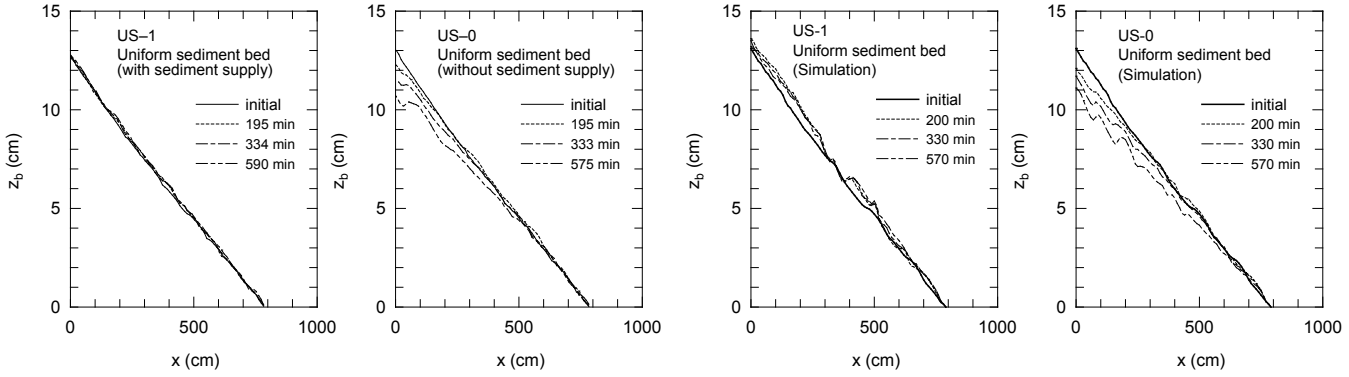

Case US-1 Case US-0 Case US-1 Case US-0

(a) Experiment (b) Simulation

Figure 3. Temporal variations in transversely averaged bed profile in experiments and simulations.

ment supply rate. In Case US-0 without sediment supply, the bed degradation progresses gradually from upstream. During the experiments, the degradation of the bed reaches approximately x = 500 cm. It was found to be that the simulation results reproduced the tendencies of the experimental results except the longitudinal profile between the initial and the t = 200 minutes and after in Case US-1.

4.2 *Low-flow channel formation process*

Figure 4 shows the temporal changes in the bed topography and sediment path in the experiment. The datum level of the bed (x=0) is an average bed level of the initial alternate bars, and the degradation and aggradation are indicated by the positive and negative value, respectively. The parts enclosed by the solid line indicate the emergent bar, and the arrow lines show the direction of sediment transport that was obtained from the experimental observation.

According to the experimental observation, the flow from the pool toward the bar-front was predominant after starting of the experiment, and the bar-front stretched to the downstream and the wavelength increased. Although the riverbed had still been submerged at then, sediments were not transported on the high area of the bed. These tendencies could be find in both Case US-1 and Case US-0. In Case US-1, however, alternate bars begun to be deformed by the concentration of the flow due to the local scour, the high areas of the bed emerged from the water surface (t=34 and 67 min.). After that, emergent bars appeared with deforming alternate bars, shallow low-flow channels were formed. Since the emergent bars were eroded easily, the low-flow channels were shifted to the downstream. The further deformation of alternate bars was caused by this shift, and new emergent bars appeared. Therefore, the emergent bars were unstable, and repeated appearance and disappearance. The low-flow channels fluctuated because of the instability of the emergent bars. In Case US-0, the high areas of the bed had emerged from the water surface at 30 minutes after starting of the experiment. The increase of wavelength and the many emergent bars could be identified at 63 minutes. In particular, the emergent bar (1) became stable due to the bed degradation of the opposite side of its bar. The bed degradation progressed from the upstream with the passage of time, simultaneously the low-flow channel there became stable. That is, a low-flow channel was formed clearly by the stable emergent bar (1) and the newly formed emergent bar (2) at 195 minutes. The low-flow channel became stable from the upstream gradually together with the bed degradation. On the other hand, the emergent bars in the downstream repeated appearance and disappearance as well as the case with the sediment supply, the low-flow channels fluctuated.

The simulation results of temporal changes in the bed topography and flow vectors are sown in Fig. 5. The vector shows the depth averaged flow velocity. The unstable emergent bars and fluctuation of low-flow channel were found to be reproduced by the numerical simulation in Case US-1 and in the lower reach of Case US-2. However, the wavelength of the low-flow channel in the upper reach of Case US-2 was shorter than that in the experiment. Sizes of emergent bars were also under-predicted. Therefore, the observed formation of flow-flow channel could not always be reproduced by the simulation.

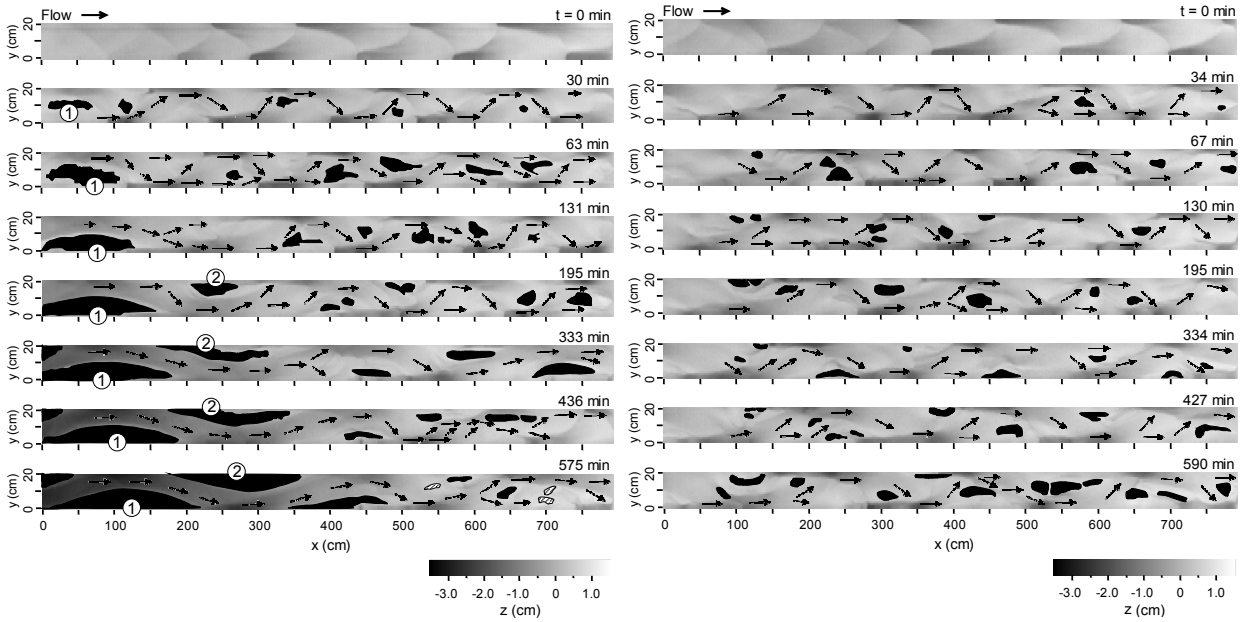

Case US-1 Case US-0

Figure 4. Temporal changes in bed topography and sediment path in experiments.

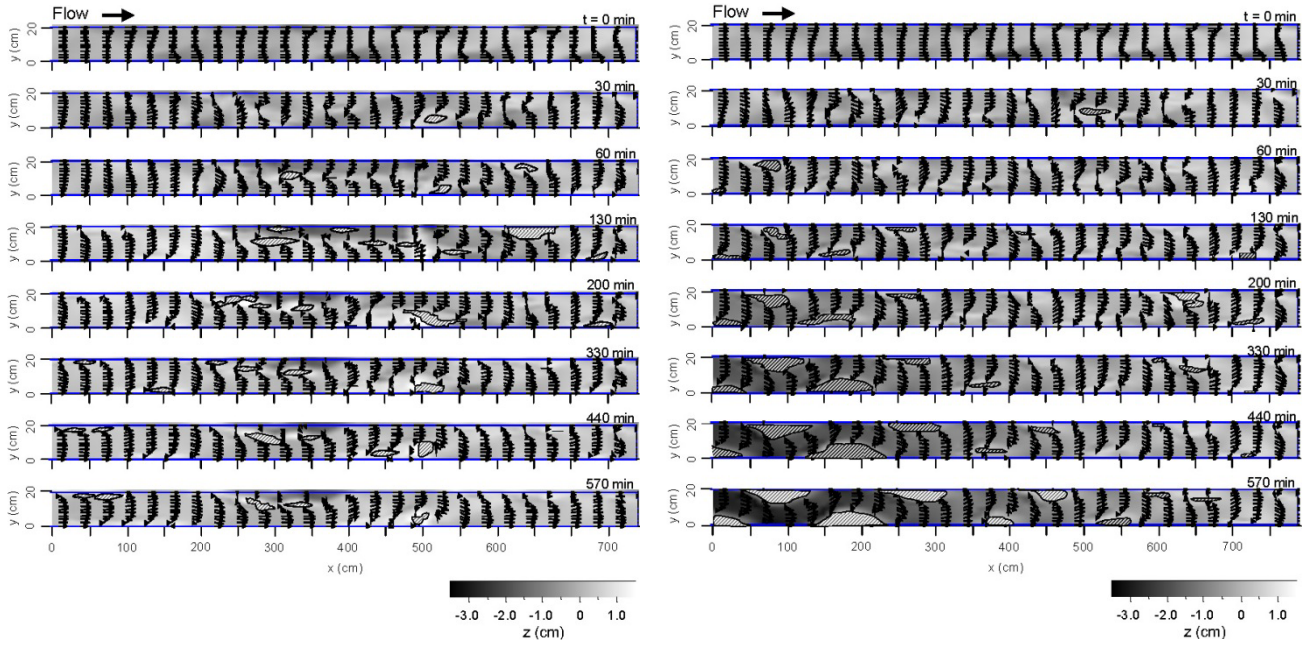

Case US-1 Case US-0

Figure 5. Temporal changes in bed topography and velocity vectors in simulation.

4.3 *Longitudinal bed profile of low-flow channel*

Figure 6 shows the temporal variations in longitudinal bed profile of low-flow channel. Shimizu et al. showed that riffles with large head and pools with small slope were formed in the low-water course through their numerical simulation. In the experiment, such riffle and pool sequence can be found in both cases. In particular, the head becomes large and pool becomes long when the low-flow channel is stable due to bed degradation (Case US-0). Such pool and riffle sequence can be observed in gravel bed rivers. The simulation results cannot always explain such sequence in Case US-1, but they can show such sequence in Case US-0. However, the riffle head and pool size are relatively small compared with the experimental results.

5 CONCLUSIONS

The results obtained in this study are summarized as follows:

1. Low-flow channels develop as a consequence of the emergent bar formation which was caused by the concentration of flow to the pools of alternate bars. In case that the river bed level did not change because of the sediment supply, the emergent bars were considerably unstable and repeated appearance and disappearance. Then, the low-flow channels were shallow and fluctuated actively. On the other hand, in case that the river bed degradation progressed because of the cutoff sediment supply, the emergent bars were stable. Then, the deep and stable low-flow channels were formed.

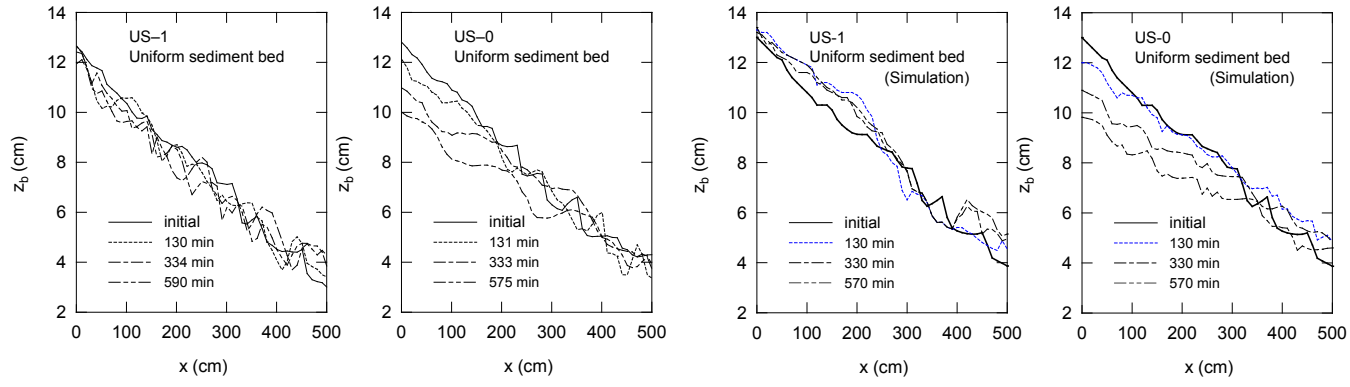

Case US-1 Case US-0 Case US-1 Case US-0

(a) Experiment (b) Simulation

Figure 6. Temporal variations in longitudinal bed profile of low-flow channel.

2. A riffle with a large head and a pool with a gentle gradient in gravel bed rivers were also found in low-flow channels which were shallow and fluctuated. Such riffle and pool sequence became stable in case that low-flow channel was deep and stable by means of the river bed degradation.
3. An individual pool moved to the downstream when the riverbed level did not change, whereas it stopped when the low-flow channel became stable.
4. The meandering wavelength of low-flow channel with river bed degradation was longer than that without it.
5. The formation process of low-flow channels observed in the experiments was found to be reproduced by the numerical simulation in both types of sediment supply. However, the meandering wavelength of low-flow channel could not always be reproduced by the simulation.

ACKNOWLEDGEMENTS

Part of this research was conducted while the author was a visiting scholar at the Ven Te Chow Hydrosystems Laboratory, the University of Illinois at Urbana-Champaign (UIUC), USA. The author expresses his deep gratitude to his research supervisor, Professor Gary Parker, Department of Civil and Environmental Engineering of UIUC, for his inspiring guidance and fruitful discussions to carry out the research.

NOTATION

a	constant for perturbation intensity
d_{16}, d_{84}	grain sizes for which 16 % and 84 % of the sediment is finer
d_m	mean grain diameter
F_r	Froude number
g	gravity acceleration
h	water depth
h_m	mean flow depth
H	mean wave height
k	depth averaged turbulent energy
L	mean wavelength
M, N	discharge flux in x and y direction
q_{bx}, q_{by}	bed-load sediment transport rates per unit width in x and y direction
q, q_m,	water discharge and mean water discharge per unit width
Q	water discharge
Q_{Bin}	sediment supply rate
$R_n(y,t)$	normal random number N(0,1)
t	time
T	duration time of experiment
u, v	velocity components in x and y direction
u_*	shear velocity
$-\overline{u'^2}$, $-\overline{u'v'}$, $-\overline{v'^2}$	depth averaged Reynolds stresses
x, y	plane Cartesian coordinates
z_b	bed elevation
κ	Kármán constant
λ	bed porosity
ν_t	kinematic eddy viscosity
ρ	fluid density
σ	sediment density
σ_g	geometric standard deviation (= $(d_{84}/d_{16})^{1/2}$)
σ_s	specific gravity
τ_b	bed shear stress
τ_{bx}, τ_{by}	bed shear stress components in x and y direction
τ_*	dimensionless bed shear stress, and
ψ	angle of repose.

REFERENCES

Ashida, K. and Michiue, M. (1972). Study on hydraulic resistance and bedload transport rate in alluvial streams. Transactions, Japan Society of Civil Engineering, No.206, 59-64 (in Japanese).

Hasegawa, K. (1983). Hydraulic Research on Planimetric Forms, Bed Topographies, and Flow in Alluvial Channels. Ph.D. Dissertation, Hokkaido University, Japan (in Japanese).
Michiue, M., Fujita, M. and Kusakabe, S. (1995). Formation of meandering streams in mountain river beds. Annual Journal of Hydraulic Engineering, JSCE, Vol. 39, pp. 613-618 (in Japanese).
Miwa, H., Daido, A. and Yokogawa, J. (2004a). Deformation of meandering streams and formation of alternate bars. Annual Journal of Hydraulic Engineering, JSCE, Vol. 48, pp. 1021-1026 (in Japanese).
Miwa, H., Daido, A. and Yokogawa, J. (2004b). Effects of water discharge on meandering streambed deformation and alternate bar formation. Proceedings of the 6th International Conference on Hydro-Science and Engineering, CD-ROM.
Miwa, H., Daido, A. and Katayama, T. (2007). Effects of water and sediment discharge conditions on variation in alternate bar morphology. Annual Journal of Hydraulic Engineering, JSCE, Vol. 51, pp. 1051-1056 (in Japanese).
Miwa, H. and Parker, G. (2012). Numerical simulation of low-flow channel evolution due to sediment augmentation. International Journal of Sediment Research, Vol.27, No.3, pp.351-361.
Nagata, N. (1999). Numerical analysis of two-dimensional unsteady flow using a general coordinate system. Lecture collection of the Short Course on Computer Simulation in Hydraulic Engineering, JSCE, pp.61-76 (in Japanese).
Nagata, N., Hosoda, T. and Muramoto, Y. (2000). Numerical analysis of river channel process with bank erosion. Journal of Hydraulic Engineering, ASCE, Vol.126, No.4, pp.243-252.
Nezu, I. and Nakagawa, H. (1993). Turbulence in Open Channel Flows, Turbulence in open channel flows. IAHR Monograph, Balkema, Rotterdam, pp.53-56.
Shimizu, Y., Osada, K. and Takanashi, T. (2004). Numerical study on formation of low-water course in a straight channel woth alternate bars. Annual Journal of Hydraulic Engineering, JSCE, Vol. 48, pp. 1027-1032 (in Japanese).
Takahata, T. and Izumi, N. (2011). Linear stability analysis of fluvial bars with bed aggradation and degradation. Annual Journal of Hydraulic Engineering, JSCE, Vol. 55, pp. S865-D870 (in Japanese).
Uchijima, K. and Hayakawa, H. (1987). Characteristics deformation of alternate bars due to low flow, Proceedings of the 31st Japanese Conference on Hydraulics, JSCE, Vol. 31, pp. 683-688 (in Japanese).
Yuki, T., Ahida, K., Egashira, S. and Okabe, K. (1992). Formation and transformation mechanism of low-waterway, Annual Journal of Hydraulic Engineering, JSCE, Vol. 36, pp. 75-80 (in Japanese).